Changes in the Hydration States of Poly(*N*-alkylacrylamide)s during Their Phase Transitions in Water Observed by FTIR Spectroscopy†

Yasushi Maeda,* Tomoya Nakamura, and Isao Ikeda

Department of Applied Chemistry and Biotechnology, Fukui University, Fukui 910-8507, Japan

Received July 25, 2000; Revised Manuscript Received November 14, 2000

ABSTRACT: Phase transitions of poly(*N*-*n*-propylacrylamide) (PnPA), poly(*N*-isopropylacrylamide) (PiPA), and poly(*N*-cyclopropylacrylamide) (PcPA) in H_2O and D_2O were investigated by Fourier transform infrared (FTIR) spectroscopy. IR spectra of these solutions were measured as a function of temperature (T) both in the heating and cooling processes. Subtraction of a spectrum at starting temperature (T_0) from a spectrum at T gives an IR difference spectrum (ΔA_{T-T_0}). The magnitudes of ΔA_{T-T_0} for IR absorption bands attributable to the alkyl and amide groups of these polymers critically increased at their lower critical solution temperatures (LCSTs). Redshifts of the amide II, C−H stretching, and C−H deformation bands were observed during the coil-to-globule transitions of these polymers. The amide I′ bands of *N*-deuterated amide groups (−CON*D*−) in PnPA and PiPA measured below their LCSTs could be fitted with single Gaussian components centered at 1630 and 1625 cm^{-1}, respectively. In contrast, two components were observed in the solutions of PnPA (1630 and 1650 cm^{-1}) and PiPA (1625 and 1650 cm^{-1}) above their LCSTs. The low-frequency and high-frequency components of the amide I′ bands of PnPA and PiPA can be attributed to the carbonyl groups that form hydrogen bonds with water (C═O···D−O−D, polymer−water hydrogen bond) and with the amide N−D groups on the polymers (C═O···D−N, polymer−polymer hydrogen bond), respectively. The molar fractions of the C═O···D−N species in the globule states were estimated to be 0.30 and 0.13 for PnPA and PiPA, respectively. Although the phase transition temperatures of PnPA solutions depend on the polymer concentration, the fractions of the C═O···D−N species are independent of the concentration (5−20 wt %), suggesting that the states of globules of PnPA at different polymer concentrations are identical with respect to hydration and water contents. The change in the profiles of the amide I′ band of PcPA during the phase transition was quite different from those of PnPA and PiPA. Although the amide I′ band of PcPA observed below the LCST was composed of a single component that could be assigned to the C═O···D−O−D species at 1634 cm^{-1}, the IR absorptions at the higher (ca. 1667 cm^{-1}) and lower (ca. 1600 cm^{-1}) wavenumbers increased above the LCST. The hydrogen bonding states about the C═O group of PcPA in the globule state are suggested to be different from those of PnPA and PiPA. As for effects of salts on the phase transition, although the LCSTs of the polymers linearly decreased and the heats of transition (ΔH) slightly decreased with an increase in NaCl concentration, NaCl had no influence on the profiles of the IR spectra of these polymers. Moreover, linear relationship between the parameters that represent the strength of anion−water interactions and the LCSTs of the polymer solutions containing one of the potassium halides (KF, KCl, KBr, and KI) was observed. The effects of ions on the LCSTs of the polymers can be explained by the strength of the interactions between the ions and water.

Introduction

Aqueous solutions of some water-soluble polymers have lower critical solution temperatures (LCSTs), and above these temperatures, the solutions separate into two phases and become turbid. Prominent examples of such polymers are poly(*N*-alkylacrylamide)s and poly(*N*-alkylmethacrylamide)s. Poly(*N*-isopropylacrylamide), in particular, has been extensively studied from both basic and technological[1] points of view in the last two decades. The macroscopic phase separations of aqueous solutions of poly(*N*-alkylacrylamide)s are accompanied by large conformational changes in the polymers, called coil−globule transitions,[2] in which the polymer chains are dehydrated and attractive interactions between polymer segments lead to the collapse of the polymer coils to a globular conformation. In contrast to the LCST behavior of polymers in organic solvents, such as the phase transition of polystyrene in cyclohexane, the coil-to-globule transition in aqueous solutions are endothermic because of the associated changes in the hydrogen bonding structure of water. Changes occurring in the structures and properties of the polymers and surrounding water molecules upon the phase transitions have been investigated by a wide variety of techniques including fluorescence,[3] Raman,[4] NMR,[5] and ESR spectrocopies;[6] calorimetry;[7] light scattering;[8] neutron scattering;[9] and dielectric relaxation.[10] Although most of the studies have centered on poly(*N*-isopropylacrylamide) (PiPA), several studies have also been carried out on poly(*N*-*n*-propylacrylamide) (PnPA) and poly(*N*-cyclopropylacrylamide) (PcPA).[11] Despite the similarities in the structures of these poly(*N*-propylacrylamide)s, their phase transition behaviors, such as the dependencies of transition temperatures on the polymer concentration and the sharpness of the temperature responsiveness, are different. As for the volume phase transitions of the gels of these polymers, the PcPA gel undergoes a continuous volume change at 40−50 °C, but the PnPA and PiPA gels show discontinuous volume phase transitions around 25 and 35 °C, respectively.[11d] These differences in their behaviors are considered to arise from small differences in the hydrations of their propyl groups.

* Author to whom correspondence should be addressed.

† Presented at the 49th Annual Meeting of the Society of Polymer Science, Japan, in May 2000.

10.1021/ma001306t CCC: $20.00
Published on Web 02/03/2001

Recently, we reported FTIR spectroscopic investigation on the coil−globule transition of aqueous solutions of PiPA.[12] IR spectroscopy was shown to be a quite suitable method for observing changes in the hydration states of individual chemical groups on the polymer chain upon transition. In particular, the analysis of the amide I band, which is mainly due to C═O stretching vibration, was shown to provide important information concerning the hydrogen bonding of the C═O group. In short, the amide I band of PiPA observed below the LCST contained a single component (1625 cm^{-1}) attributable to C═O···H−O (polymer−water hydrogen bonding), whereas a second component (1650 cm^{-1}) due to C═O···H−N (polymer−polymer hydrogen bonding) appeared above the LCST. Moreover, changes in the C−H stretching IR bands indicated the dehydration of the isopropyl group upon the transition.

The intention of the present study is to investigate differences in the hydration of PnPA and PcPA compared to that of PiPA in both the coil and the globule states. The hydrogen bonding of the amide groups and the hydrophobic hydration of alkyl groups are analyzed by IR spectroscopy, and the relationship between changes in the hydration states and the heat of transition will be discussed.

Experimental Section

Materials. *N*-Isopropylacrylamide (iPA, Kohjin) was purified by recrystallization from benzene−*n*-hexane. *N*-*n*-Propylacrylamide was synthesized via coupling of acryloyl chloride (Wako Pure Chemicals) and *n*-propylamine (Wako) in benzene and purified by distillation at 91 °C (1.5 mmHg). The chemical structure of nPA was confirmed by ^{1}H NMR spectroscopy: δ_H (500 MHz, $CDCl_3$) = 0.95 (t, 3H, C*H*$_3$), 1.57 (m, 2H, C*H*$_2$CH$_3$), 3.31 (m, 2H, C*H*$_2$CH$_2$CH$_3$), 5.63 (m, 2H, C*H*$_2$═CH), 6.09 (m, 1H, CH$_2$═C*H*), 6.28 (m, 1H, N*H*). *N*-Cyclopropylacrylamide (cPA) was synthesized via coupling of acryloyl chloride and cyclopropylamine (Wako) in benzene and purified by recrystallization from benzene−*n*-hexane. The chemical structure of cPA was confirmed by ^{1}H NMR: δ_H (400 MHz, $CDCl_3$) = 0.68 (d, 4H, C*H*$_2$), 2.80 (m, 1H, C*H*−N), 5.76 (d, 1H, C*H*═CH$_2$), 6.07 (m, 2H, C*H*$_2$═CH), 6.27 (d, 1H, CH$_2$═C*H*), 6.28 (m, 1H, N*H*). Poly(*N*-*n*-propylacrylamide) (PnPA), poly(*N*-isopropylacrylamide) (PiPA) and poly(*N*-cyclopropylacrylamide) (PcPA) were synthesized via radical polymerization in methanol at 70 °C for 7 h using 2,2′-azobis(isobutyronitrile) as an initiator. After evaporation, the polymers were precipitated from acetone−*n*-hexane. The polymers obtained were purified by dialysis (seamless cellulose tube, exclusion limit of 8000) and lyophilized. To prepare *N*-deuterated PnPA [(−CH$_2$−CH(CONDnPr)-)$_n$, PnPA-d], PiPA [(−CH$_2$−CH(CONDiPr)-)$_n$, PiPA-d], and PcPA [((−CH$_2$−CH(CONDcPr)-)$_n$, PcPA-d], the corresponding polymers dissolved in D_2O (EURIS-TOP, 99.9%) were allowed to stand for more than 1 day below their LCSTs to equilibrate H−D exchange and were then lyophilized. To distinguish them from PnPA-d, PiPA-d, and PcPA-d, the undeuterated counterparts are denoted PnPA-h, PiPA-h, and PcPA-h, respectively. Roughly estimated molecular weights of the polymers were determined by gel permeation chromatography [Toso HLC-803D; column, Toso G3000PW (30 cm) + G5000PWXL (30 cm); mobile phase, water (1.0 mL $mmin^{-1}$); poly(ethyleneglycol)s were used as standard samples] as 11 000 and 700 000 for PiPA and PcPA, respectively. The molecular weight of PnPA determined from the intrinsic viscosity in water at 10 °C $\{[\eta] = (1.69 \times 10^{-2})M_w^{0.678}\}$[11b] was 140 000.

The monomer analogues, *N*-*n*-propylpropionamide (nPPA), *N*-isopropylpropionamide (iPPA), and *N*-cyclopropylpropionamide (cPPA), were synthesized via coupling of propionyl chloride and the corresponding propylamines in benzene and purified by distillation (nPPA, cPPA) or recrystallization in benzene−*n*-hexane (iPPA). ^{1}H NMR: nPPA, δ_H (400 MHz, $CDCl_3$), 1.25 (m, 6H, C*H*$_3$), 1.74 (m, 2H, C*H*$_2$−CH$_2$), 2.39 (d, 1H, C*H*$_2$−C═O), 3.43 (m, 2H, C*H*$_2$−N), 5.63 (s, 1H, NH−C*H*$_2$−), 6.28 (m, 1H, N*H*); iPPA, δ_H (400 MHz, $CDCl_3$), 1.15 (t, 9H, C*H*$_3$), 2.18 (m, 2H, C*H*$_2$−C═O), 4.08 (m, 1H, C*H*−N), 5.35 (s, 1H, N*H*); cPPA, δ_H (400 MHz,$CDCl_3$), 0.70 (d, 6H, C*H*$_2$), 1.15 (t, 3H, C*H*$_3$−), 2.71 (m, 1H, C*H*−N), 6.05 (s, 1H, N*H*).

Turbidimetry. The turbidity of an aqueous polymer solution (0.5 wt %) was followed by the absorbance at 500 nm using a spectrophotometer (UV200-100, Hitachi). The temperature of quartz observation cell was continuously raised by a circulating water bath (BU150S, Yamato) at a rate of ca. 1 °C/min. The temperature of the polymer solution was measured using an electronic thermometer (SK-L200T, Sato Keiryoki) with a thermistor sensor. The absorbance and temperature measurements of the polymer solution were simultaneously collected by a computer (PC-9821Ce, NEC) via an A/D converter [AD12-8J(98), Contec] and analyzed with a homemade program.

Differential Scanning Calorimetry (DSC). DSC measurements were performed using a Micro Calorimetry System (MicroCal Inc.) with a scanning rate of 0.75 °C/min both in the heating and cooling processes. The polymer sample dissolved in H_2O (0.5 wt %) was degassed and transferred to the sample cell (cell volume = 1.22 mL) with a syringe. An identical volume of the solvent of the same composition was placed in the reference cell. Data analyses were carried out with Origin software (MicroCal).

FTIR Measurements. IR spectra were measured using a Jasco FTIR-620 spectrometer equipped with a TGS detector. The polymer sample dissolved in D_2O or H_2O (typically 20 wt %, 50 μL) was incubated for >12 h below the LCST to equilibrate. A volume of 10 μL of the solution was pipetted into an IR cell with two CaF_2 windows (ϕ 20 × 2 mm) and a spacer (10 μm thick). The IR cell was attached to a metal cell holder, and the temperature was continuously increased or decreased with a circulating water bath (BU150S, Yamato) at a rate of ca. 1 °C/min. The background spectrum for one cycle of the measurement was obtained with a sample solution in the IR cell equilibrated at the starting temperature (T_0). Then, time-resolved IR spectra were continuously collected at a resolution of 2 cm^{-1} with a rate of one single-scan spectrum per second, and every 30 single-scan spectra were averaged. The temperature of the cell holder was simultaneously measured by SK-L200T thermometer. The IR difference spectrum given by the differences in IR absorption intensities (A) measured at T and the starting temperature (T_0) is designated as ΔA_{T-T_0}. Analyses of the IR spectra such as Fourier self-deconvolution, curve fitting, and baseline subtraction were performed with Spectra Manager software (Jasco).

Results and Discussion

Phase Transitions and IR Spectra of Aqueous Solutions of Poly(*N*-alkylacrylamide)s. Figure 1a shows the IR absorption spectra of PnPA-h in H_2O and PnPA-d in D_2O measured at 15.0 °C. The prominent IR bands are C−H stretching bands, amide bands, and C−H deformation bands. The IR frequencies and assignments of the observed peaks are compiled in Table 1. Because the amide II band contains a contribution from the N−H bending vibration (60%), the band was sensitive to deuteration and shifted from 1561 cm^{-1} for PnPA-h to 1470 cm^{-1} for PnPA-d. Other bands were insensitive to deuteration. For clarity, the amide bands for *N*-deuterated species (−COND−) are denoted as amide I′ and amide II′. The main advantage of using D_2O as a solvent is a shift in the deformation band of water to around 1200 cm^{-1}, which prevents the band from overlapping the amide I′ band of the polymer.

The differential IR spectra (ΔA_{29-15}) of PnPA-h and PnPA-d obtained by subtraction of the IR absorption spectra measured below the LCST (15.0 °C) from those measured above the LCST (29.0 °C) are shown in Figure

Table 1. Observed IR Frequencies (in cm^{-1}) and Assignments of PnPA-h and PnPA-d

PnPA-h				PnPA-d		
H_2O solution	IR difference band in H_2O solution	neat	assignment	D_2O solution	IR difference band in D_2O solution	neat
2973	2983 (−), 2961 (+)	2964	antisymmetric C−H stretch of $-CH_3$	2971	2980 (−), 2962 (+)	2964
2943	2946 (−), 2927 (+)	2934	antisymmetric C−H stretch of $-CH_2-$	2941	2946 (−), 2927 (+)	2934
2882	2885 (−), 2874 (+)	2875	symmetric C−H stretch of $-CH_3$	2882	2885 (−), 2874 (+)	2875
ov[a]	ov[a]	1642	amide I	1632	1654 (+), 1632 (−)	1642
1568	1573 (−), 1541 (+)	1550	amide II	1477	1483 (−), 1457 (+)	1462
1462	1463 (−), 1457 (+)	1459	C−H deformation	ov[a]	ov[a]	ov[a]
1446	1447 (−), 1437 (+)	1443	C−H deformation	1446	1446 (−), 1436 (+)	1438
1386	1387 (−), 1379 (+)	1383	C−H deformation	1386	1387 (−), 1379 (+)	1381
1372	1374 (−), 1363 (+)	1362	amide III	−	−	−
1348	1348 (−), 1343 (+)	1345	C−H deformation	1348	1348 (−), 1343 (+)	1345

[a] ov = overlap with other band.

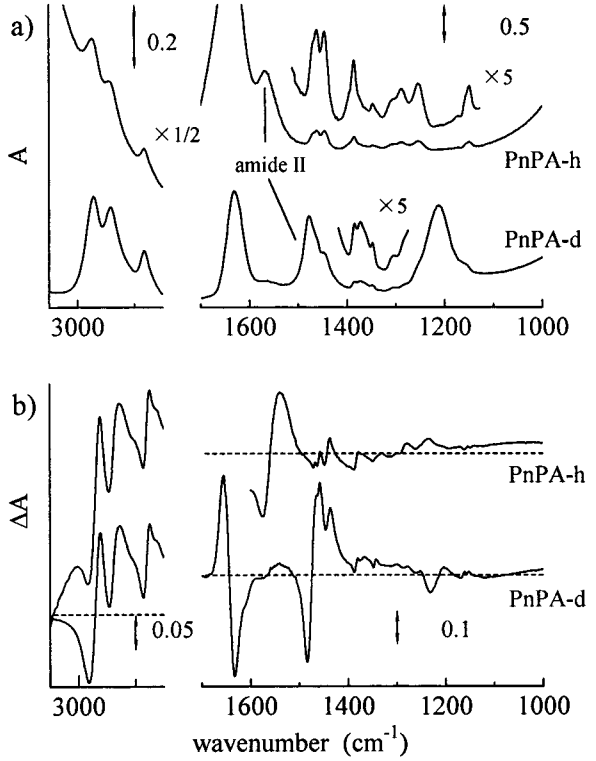

Figure 1. (a) IR absorption spectra of PnPA-h in H_2O and PnPA-d in D_2O at 15.0 °C. (b) IR difference spectra (ΔA_{29-15}) induced by the phase transition of PnPA-h in H_2O and PnPA-d in D_2O.

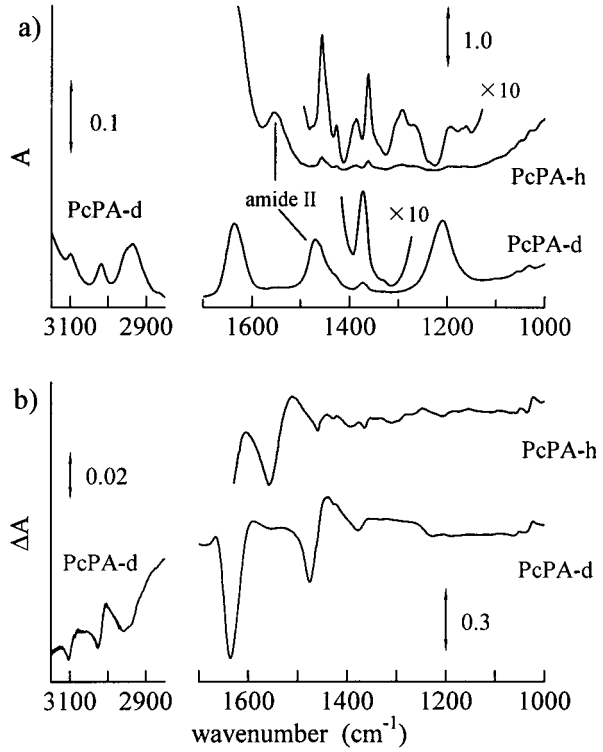

Figure 2. (a) IR absorption spectra of PcPA-h in H_2O and PcPA-d in D_2O at 40 °C. (b) IR difference spectra (ΔA_{60-40}) induced by the phase transition of PcPA-h in H_2O and PcPA-d in D_2O.

1b. The magnitudes of the IR difference spectra of PnPA-h and PnPA-d are much larger than those of PiPA-h and PiPA-d measured in the same temperature region (15.0−29.0 °C), where PiPA shows no transition phenomena. The contribution of simple temperature effects, which also might cause the shift and broadening of IR bands, to the profiles of the IR bands seems to be much smaller than those of the phase transition. In the IR difference spectra, negative bands are associated with IR absorption by the polymer in the coil state, and positive bands represent absorption in the globule state. The appearance of both positive and negative peaks for each vibration mode of PnPA means that changes in the conformation and/or interactions of the corresponding chemical groups take place during the phase transition. For example, a pair of IR difference peaks observed at 2983 cm^{-1} (negative) and 2961 cm^{-1} (positive) are due to a redshift of the antisymmetric C−H stretching band of the methyl group during the transition. Most of the IR bands of PnPA show redshifts upon the transition, with the exception of the amide I band, which shifted from 1632 to 1654 cm^{-1}.

The IR absorption and difference spectra of PcPA-h in H_2O and PcPA-d in D_2O are shown in Figure 2, and the IR frequencies and assignments are compiled in Table 2.

To show the progress of the phase transition, the difference between ΔA_{T-T_0} at the positive peak and that at the negative peak of a vibration mode in a difference spectrum $[\Delta\Delta A_{T-T_0}(\nu_1,\nu_2)]$ is plotted against temperature. The value of $\Delta\Delta A_{T-T_0}(\nu_1,\nu_2)$ is defined as

$$\Delta\Delta A_{T-T_0}(\nu_1,\nu_2) = \Delta A_{T-T_0}(\nu_1) - \Delta A_{T-T_0}(\nu_2)$$

where ν_1 and ν_2 denote the wavenumbers of the positive and negative peaks, respectively, and the subscripts T and T_0 are the temperatures of the spectral measurements. If we define ν_1 to be lower than ν_2, a positive value of $\Delta\Delta A_{T-T_0}(\nu_1,\nu_2)$ means a redshift of the corresponding IR absorption band during the phase transi-

Table 2. Observed IR Frequencies (in cm^{-1}) and Assignments of PcPA-h and PcPA-d

PcPA-h				PcPA-d		
H_2O solution	IR difference band in H_2O solution	neat	assignment	D_2O solution	IR difference band in D_2O solution	neat
ov[a]	ov[a]	3089	antisymmetric C−H stretch of cyclopropyl	3100	3103 (−), 3079 (+)	3089
ov[a]	ov[a]	3008	symmetric C−H stretch of cyclopropyl	3020	3025 (−), 3003 (+)	3010
ov[a]	ov[a]	2945	antisymmetric C−H stretch of $-CH_2-$	2955	2960 (−), 2950 (+)	2949
ov[a]	ov[a]	2927	symmetric C−H stretch of $-CH_2-$	2934	2937 (−), 2922 (+)	2929
ov[a]	ov[a]	1645	amide I	1635	1667 (+), 1635 (−), 1600 (+)	1645
1554	1554 (−), 1509 (+)	1537	amide II	1470	1475 (−), 1443 (+)	1456
1457	1459 (−), 1440 (+)	1454	C−H deformation	ov[a]	ov[a]	ov[a]
1427	1429 (−), 1420 (+)	1425	C−H deformation	ov[a]	ov[a]	ov[a]
1388	1392 (−), 1376 (+)	1382	amide III	−	−	−
1362	1364 (−), 1351 (+)	1362	C−H deformation	1371	1373 (−), 1365 (+)	1369
1031	1035 (−), 1023 (+)	1023	C−H deformation	1032	1043 (−), 1022 (+)	1024

[a] ov = overlap with other band.

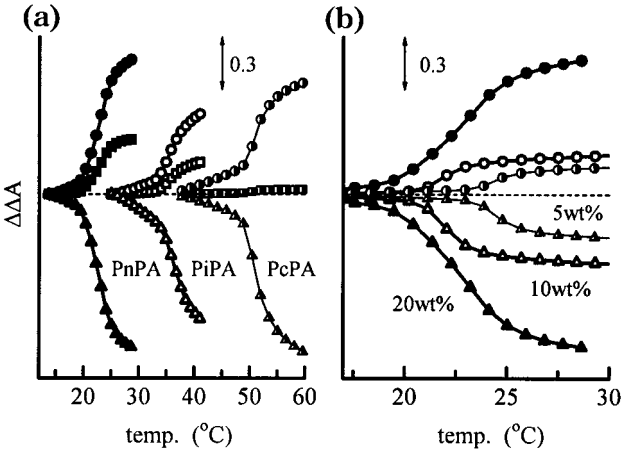

Figure 3. (a) Differences in IR absorption of the positive and negative peaks [$\Delta\Delta A_{T-T_0}(\nu_1,\nu_2)$] of selected vibration modes in the IR difference spectra (ΔA_{T-T_0}) induced by the phase transition of PnPA-d (solid marks), PiPA-d (open marks), and PcPA-d (half-solid marks) in D_2O are plotted against temperature. ●, ○, ◑: $\Delta\Delta A_{T-T_0}$(amide II′). ▲, △, ◭: $\Delta\Delta A_{T-T_0}$(amide I′). ■, □, ◨: $\Delta\Delta A_{T-T_0}(\nu C-H)$. (b) Differences in IR absorption of the positive and negative peaks [$\Delta\Delta A_{T-T_0}(\nu_1,\nu_2)$] of selected vibration modes in the IR difference spectra (ΔA_{T-T_0}) induced by the phase transition of PnPA-d in D_2O at 5 (solid marks), 10 (open marks), and 20 wt % (half-solid marks) are plotted against temperature. ●, ○, ◑: $\Delta\Delta A_{T-T_0}$(amide II′). ▲, △, ◭: $\Delta\Delta A_{T-T_0}$(amide I′).

tion in a heating process. Values of $\Delta\Delta A_{T-25}(\nu_1,\nu_2)$ for the C−H stretching and amide I′ and II′ vibration modes of PnPA, PiPA, and PcPA are plotted against temperature in Figure 3. For instance, because the amide I′ mode has a positive peak at 1654 cm^{-1} and a negative peak at 1632 cm^{-1}, as shown at the bottom of Figure 1b, the values of $\Delta\Delta A_{T-15}$(1632,1654) are plotted as solid triangles in Figure 3a. The onsets of an increase or decrease in $\Delta\Delta A_{T-15}(\nu_1,\nu_2)$ curves for PnPA were observed at around 20 °C, and the values grew in the temperature range of 20−29 °C. $\Delta\Delta A_{T-T_0}(\nu_1,\nu_2)$ curves for PiPA and PcPA have onsets at around 34 and 49 °C, respectively. The gradual growth in the values of $\Delta\Delta A$ with increasing temperature below the LCST is due to simple temperature effects, which cause slight shifts in the IR bands, accompanied by broadening. There is a considerable difference in the LCSTs of PnPA, PiPA, and PcPA, despite their similar chemical compositions. The size of the hydrophobic hydration shell and the extent of the decrease in the entropy of water expand with an increase in the solvent accessible surface area (A_{sf})[13] of the alkyl group. A_{sf} of an *n*-propyl group is the largest among the alkyl groups, and the surface area of isopropyl group is larger than that of cyclopropyl group. A larger A_{sf} for a hydrophobic group is associated with a larger decrease in the entropy of the solvent water when this group is dissolved in water. A decrease in the entropy of water to the largest extent might be the main reason that the LCST of PnPA is the lowest among these polymers. In addition to the smallest A_{sf}, the strain of the bond angles of the cyclopropyl group reduces the overlap of the electron clouds and makes the cyclopropyl group more hydrophilic compared to the isopropyl group, resulting a higher LCST for PcPA than for PiPA. The $\Delta\Delta A_{T-T_0}(\nu_1,\nu_2)$ curves shown in Figure 3 were measured in D_2O. The transition temperatures of the three polymers in H_2O were slightly (about 1 °C) lower than those in D_2O. For PiPA and PcPA, the onsets observed in the $\Delta\Delta A_{T-T_0}(\nu_1,\nu_2)$ curves are close to their transition temperatures determined by cloud point and DSC measurements despite the large difference in the polymer concentratios (IR, 20 wt %; turbidimetry and DSC, 0.5 wt %). In contrast, the LCST of PnPA exhibited a prominent concentration dependence, as shown in Figure 3b. The larger concentration dependence of PnPA than of PiPA was also observed by DSC measurements previously.[11d]

Change in the Amide Bands of Deuterated Poly(*N*-alkylacrylamide)s during the Phase Transition. The amide I′ bands of the polymers in D_2O were analyzed in more detail. The amide I mode contains contributions from the C═O stretching vibration (about 80%), with a minor contribution from the C−N stretching vibration. The lone-pair electrons on the oxygen atom of the C═O can accept hydrogen from water or the amide N−H and form a hydrogen bond. The strength of the hydrogen bond correlates with the frequency of the amide I mode, that is, the stronger the hydrogen bond involving the amide C═O, the lower the electron density in the C═O group and the lower the amide I frequency. The profiles of the amide I′ bands of PiPA-d and PnPA-d measured in the transition temperature region showed isosbestic behaviors, that is, IR absorption at higher-wavenumber side of isosbestic points (PiPA, 1637 cm^{-1}; PnPA, 1644 cm^{-1}) increased and absorption at lower-wavenumber side decreased with increasing temperature. The isosbestic behaviors indicate the existence of two distinct components, whose positions and line shapes are independent of temperature but whose intensities change. As shown in Figure 4, the amide I′ band of each polymer observed below the LCST consisted of a single component (component 1). The peak maxima of the component were 1630 cm^{-1} for PnPA and 1625 cm^{-1} for PiPA. The amide I′ bands

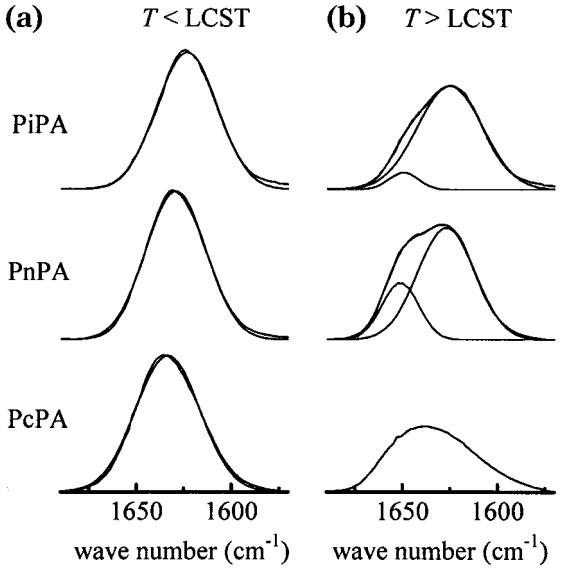

Figure 4. (a) Baseline-subtracted amide I′ bands of PnPA-d (13.2 °C), PiPA-d (24.9 °C), and PcPA-d (33.0 °C) below their LCSTs and a best-fit single Gaussian component (PnPA, center = 1630 cm^{-1}, width at half-height (W_h) = 37 cm^{-1}; PiPA, center = 1625 cm^{-1}, W_h = 37 cm^{-1}; PcPA, center = 1634 cm^{-1}, W_h = 40 cm^{-1}). (b) Baseline-subtracted amide I′ bands of PiPA-d (41.0 °C), PnPA-d (29.0 °C), and PcPA-d (61.0 °C) above their LCSTs and two Gaussian components (PnPA, center = 1630 cm^{-1}, width at half-height (W_h) = 32 cm^{-1} and center = 1650 cm^{-1}, W_h = 23 cm^{-1}; PiPA, center = 1625 cm^{-1}, W_h = 33 cm^{-1} and center = 1650 cm^{-1}, W_h = 17 cm^{-1}).

Table 3. Observed IR Frequencies (in cm^{-1}) of Amide I′ Bands of nPPA-d, iPPA-d, and cPPA-d

	position of amide I′ band (cm^{-1})		
	D_2O solution		
	1 wt %	10 wt %	neat
nPPA-d	1608	1614	1649
iPPA-d	1603	1608	1643
cPPA-d	1610	1616	1653

of PnPA and PiPA measured above their LCSTs could be fitted with two components as predicted by the isosbestic behaviors. The position of the second components is 1650 cm^{-1} for both PnPA and PiPA (component 2). Because the frequency of component 2 is higher than those of component 1, the C═O species that gives rise to component 2 forms a weaker hydrogen bond than the C═O species that is responsible for component 1.

To assign these components of the amide I band of poly(*N*-alkylacrylamide)s, we analyzed the positions of the amide I bands of the monomer analogues (nPPA, iPPA, and cPPA) in D_2O at various concentrations (Table 3). The amide I′ bands of nPPA, iPPA, and cPPA in dilute solutions (1 wt %) are observed at 1608, 1603, and 1610 cm^{-1}, respectively, with most of the amide groups considered to form hydrogen bonds with the solvent water. The wavenumbers of the amide I′ bands of these analogues decrease in the order cyclopropyl > *n*-propyl > isopropyl, which is the same order of the wavenumbers for the corresponding polymers measured below their LCSTs. Because the carbonyl carbons of these analogues connect to a methylene carbon and those of the poly(*N*-alkylacrylamide)s bind to a methine carbon, the electron densities on the C═O bonds of the poly(*N*-alkylacrylamide)s are higher than those of the corresponding monomer analogues, and therefore, the wavenumbers of the amide I′ bands of the polymers are

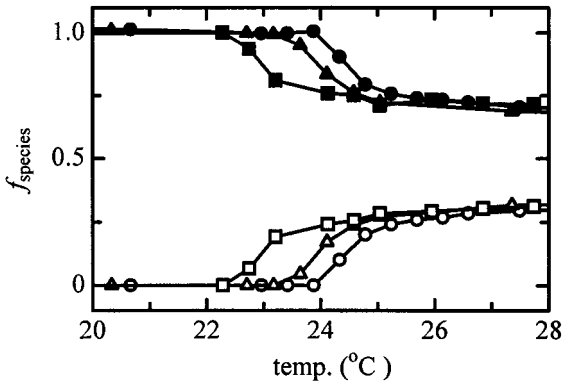

Figure 5. Molar fractions of C═O groups of PnPA-d that forms hydrogen bonds with water (C═O···D−O−D, solid marks) and N−D groups (C═O···D−N, open marks) in D_2O solution ($f_{species2}$) is plotted against temperature. [PnPA-d] = 20 wt % (■, □), 10 wt % (▲, △), and 5 wt % (●, ○).

higher than those of the analogues. The positions of the amide I′ bands of the analogues shift to higher wavenumbers with increasing concentration, probably because the fractions of the amide−amide hydrogen bonds (C═O···D−N) increase. In the neat solids or liquids of the analogues, the C═O···D−N hydrogen bonds are dominant and the amide I′ bands of nPPA, iPPA, and cPPA appear at 1649, 1643, and 1653 cm^{-1}, respectively. Thus, the wavenumbers of the amide I′ band of the C═O···D−N species are higher than those of the C═O···D−O−D species. Although the precise positions of the amide I′ bands of the polymers are different from those of the corresponding analogues, their relative positions might be closely related. Because component 1 of the amide I′ band of PnPA and PiPA has a relatively lower wavenumber compared with component 2 and is dominant under water-rich conditions (the coil states), it could be assigned to the vibration of the C═O group that forms a hydrogen bond with water (C═O··· D−O−D, species 1). On the other hand, because component 2 has a relatively higher wavenumber and is dominant at low water contents (the globule states), it could be attributable to the C═O group that forms a hydrogen bond with the amide N−D group (C═O··· D−N, species 2).

Because the molar absorption coefficients of the two C═O species might not be the same, the relative areas of the amide I′ bands do not directly represent the molar fractions of these species. If we assume a 1:1 conversion between species 1 and species 2, then the integrated areas of component 1 and component 2 measured at various temperatures give the ratio of the molar absorption coefficients of species 2 relative to that of species 1 as 0.65 and 0.90 for PiPA and PnPA, respectively. By using these values, the molar fractions of species 1 and species 2 of PnPA were estimated at various temperatures, as shown in Figure 5. Figure 5 shows that about 30% of the C═O groups in PnPA form hydrogen bonds with the amide N−D groups of the polymer, which connect polymer chain by forming intrachain and interchain linkages, and the remaining 70% of the C═O groups form hydrogen bonds with water molecules even in the globule state. Moreover, the molar fraction of species 2 in the globule state is independent of the polymer concentration despite the remarkable concentration dependence of the LCST of PnPA. This is probably because the water contents in the globule were almost the same among these solutions (5, 10, and 20 wt %). The molar fractions of species 2 in the globules

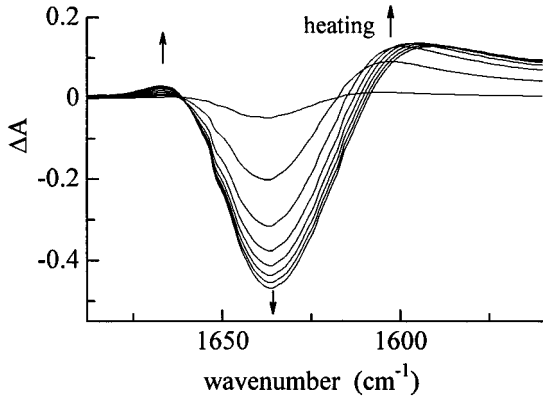

Figure 6. IR difference spectra (ΔA_{T-LCST}) at the amide I′ region of PcPA-d in D_2O induced by the phase transition. T = 49.6−60.4 °C. Arrows indicate increases in temperature.

of PiPA was previously estimated as 0.13.[12] These results indicate that a relatively small portion of the C═O groups of PiPA and PnPA are dehydrated during the coil-to-globule transition and that the majority of the C═O groups remain to form hydrogen bonds with water. Wang et al. reported that the globule of PiPA still contains ca. 66% water even in its fully collapsed state.[8a] Lele et al. predicted that the reduction in the amount of water that forms a hydrogen bond with PiPA is relatively small during the coil-to-globule transition in spite of the large decrease in the total bound water content.[14] Moreover, molecular dynamics simulations by Tamai et al. showed that no polymer−polymer hydrogen bonds (C═O···H−N) exist in 25 wt % PiPA solutions.[15] In contrast, in 50 and 75 wt % PiPA solutions (polymer concentration is higher than that in the globule), about 30% of the C═O groups form hydrogen bonds with the N−H groups with a reduction in the number of C═O···H−O−H and N−H···OH_2 hydrogen bonds. Because the total numbers of hydrogen bonds about the C═O group are shown to be almost constant, the reduction in polymer−water hydrogen bonds is compensated for by polymer−polymer hydrogen bonding.[15] These previously reported results qualitatively agree well with our current experimental results. In addition, the phase transitions of PiPA and PnPA clearly show hysteresis, that is, the transition temperature ranges for the cooling processes are slightly lower than those of the heating processes. The hysteresis means that the globule-to-coil transitions contain more time-consuming processes than the coil-to-globule transitions. The intrachain and interchain hydrogen bonds that are formed among the amide groups of these polymers in the globule states might be responsible for this hysteresis.

The change in the profiles of the amide I′ band of PcPA during the transition was quite different from those of PnPA and PiPA (Figure 6). Although the amide I′ band of PcPA-d below the LCST was composed of a single component assigned to the C═O···D−O−D species at 1634 cm^{-1}, two new components appeared at both the higher- and lower-wavenumber sides of the 1634-cm^{-1}component (ca. 1667 and 1600 cm^{-1}). With an increase in temperature, the area of the 1634-cm^{-1} component decreased and the areas of the 1670-cm^{-1} and 1600-cm^{-1} components increased. The total area of the amide I′ band of PcPA noticeably deceased in the transition temperate region. The 1670-cm^{-1} component might be due to the C═O species that forms no hydrogen bond or a very weak hydrogen bond, and the 1600-cm^{-1} component might be due to a very strongly hydrogen-bonded C═O species. However, precise assignments of these components are impossible at this moment. Our tentative results on the phase transition of poly(*N*,*N*-diethylacrylamide), which has no amide protons as a hydrogen bond donor and no ability to form polymer−polymer hydrogen bonds, shows the existence of two and three amide I′ components below and above its LCST, respectively. Considerable variety in the hydrogen bonding of the amide groups was observed among the polymers analyzed. At the present time, we can only point out a possibility that these modes of hydrogen bonding about the amide groups of these polymers play an important role in their behaviors at the coil−globule transitions, such as the susceptibility for thermal stimulus and the hysteresis.

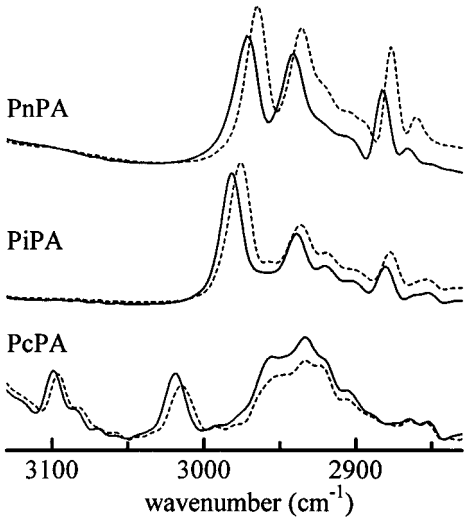

Figure 7. Fourier self-deconvoluted C−H stretching IR absorption spectra measured below (solid lines) and above the LCSTs (broken lines) of PiPA-d (24.9 and 41.0 °C), PnPA (13.2 and 29.0 °C), and PcPA (33.0 and 61.0 °C) in D_2O. The half width used for the calculation was 30 cm^{-1}.

Changes in the C−H Stretching Bands of Poly(*N*-alkylacrylamide)s during their Phase Transitions. The C−H stretching regions (2840−3000 cm^{-1}) of the IR spectra provide information concerning the hydration of the alkyl groups. Figure 7 shows the IR spectra in the C−H stretching region of PnPA, PiPA, and PcPA measured below (solid lines) and above (broken lines) their LCSTs. To make the positions of the individual IR bands clear, these spectra were Fourier self-deconvoluted. Most of the IR bands undergo redshifts during the coil-to-globule transitions. A number of experimental studies have shown that the C−H stretching band of an alkyl group undergoes a blueshift when the alkyl group interacts with water.[16] Ab initio calculations have also shown that the C−H bond contracts and its vibrational frequency undergoes a blueshift upon interaction with water.[17] The blueshift of the C−H stretching band is a marked contrast to the redshift of an X−H stretching band upon the formation of a conventional hydrogen bond (X−H···Y) such as O−H···OH_2. The discrepancy was rationalized by the difference in the magnitudes of the components of the interaction energy in the C−H···OH_2 and O−H···OH_2 interactions. The exchange force, which tends to contract the C−H bonds, is slightly larger than the forces pushing toward elongation (electrostatic, polarization, charge transfer, and dispersion) in the C−H···OH_2 interaction; therefore, the C−H bond contracts, and the C−H stretching frequency experiences a blueshift in the

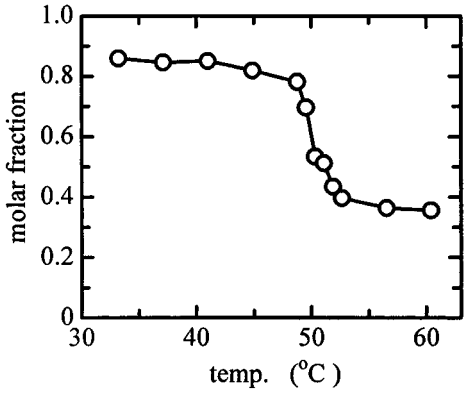

Figure 8. Molar fractions of the hydrated cyclopropyl groups of PcPA-d that give a symmetric C−H stretching band at 3020 cm^{-1} are plotted against temperature. Two Gaussian components (center = 3020 cm^{-1}, W_h = 12 cm^{-1} and center = 3013 cm^{-1}, W_h = 12 cm^{-1}) were used to deconvolute the IR bands by using a curve-fitting method. the PcPA-d concentration was 20 wt %.

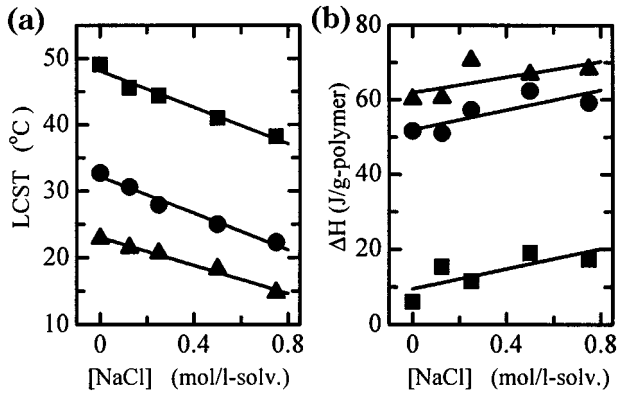

Figure 9. (a) NaCl concentration dependence of the LCSTs of PnPA (▲), PiPA (●), and PcPA (■) in H_2O determined by DSC measurements. The LCST was defined as the onset of the endothermic peak of heating process. The polymer concentration was 0.5 wt %, and the scanning rate was 0.75 °C/min. (b) NaCl concentration dependence of ΔH in the phase transitions of PnPA (▲), PiPA (●), and PcPA (■) solutions. The conditions were the same as in part a.

complex. Thus, the redshifts of the C−H stretching IR bands of poly(*N*-alkylacrylamide)s above their LCSTs observed here are indicative of the dehydration of the alkyl groups.

Because the symmetric C−H stretching band of the cyclopropyl group is isolated from the other bands, this band was analyzed in more detail. The C−H stretching band was decomposed into two components, i.e., hydrated C−H (3020 cm^{-1}) and dehydrated C−H (3013 cm^{-1}). The molar fraction of the hydrated C−H group species obtained by using a curve fitting method was critically decreased at the LCST (49 °C), as shown in Figure 8. In contrast to the amide group of PcPA, the cyclopropyl group was partially dehydrated even in the coil state and was dehydrated up to 60% in the globule state.

Effects of Ions on the LCST and IR Spectra of Poly(*N*-alkylacrylamide)s. Next, the effects of salts on the LCST, enthalpy of transition (ΔH), and IR spectra were investigated. Figure 9a shows the NaCl concentration dependence of the LCSTs of PnPA, PiPA, and PcPA determined by DSC measurements. The LCST was defined as the onset of the endothermic peak of the transition in the heating process. The LCSTs of these polymers decreased linearly with increasing NaCl concentration in this region. The similar slopes of the lines for the polymers obtained by least-squares regressions indicate that the effect of NaCl on the LCSTs was identical despite difference in the chemical properties of these polymers. The ΔH values for these polymer solutions slightly increased with NaCl concentration as shown in Figure 9b.

The values of ΔH for PnPA, PiPA, and PcPA in pure H_2O were calculated to be 6.8, 5.8, and 0.7 kJ/mol of monomer units, respectively. The value of ΔH for PiPA obtained here is close to those reported previously.[7f,7g] There are some probable processes that might consume heat during the phase transition. Some authors attributed ΔH to the breakage of hydrogen bonds between the amide group and water.[7e,7f] However, as mentioned above, most of the amide−water hydrogen bonds are retained even in the globule state, and the loss of the amide−water hydrogen bonds is compensated for by the formation of amide−amide and water−water hydrogen bonds as follows:

$$C{=}O\cdots H_2O + N{-}H\cdots OH_2 \rightarrow C{=}O\cdots H{-}N + H{-}O{-}H\cdots OH_2$$

Therefore, the contribution of the hydrogen-bond-breaking process to ΔH of the transition might be small. Saito et al.[7g] and Kim et al.[7c] attributed the heat of transition of PiPA to the destruction of water−water hydrogen bonds in the hydrophobic hydration shell around the isopropyl group. Many experiments and simulations have shown the enhancement of the formation of water−water hydrogen bonds in the hydrophobic hydration shell.[18] Above the LCST, the hydrophobic parts of the polymers are dehydrated and associate with one another through hydrophobic interactions. Because water molecules that exist in the hydrophobic hydration shell in the coil state are released to become bulk water in the globule state, the total number of water−water hydrogen bonds is reduced. ΔH for breaking an O−H···O hydrogen bond of water was reported to be ca. 12 kJ/mol.[19] If we assume that ΔH of the transition is solely consumed to break water−water hydrogen bonds, then the number of such bonds broken is estimated to be ca. 0.6, 0.5, and 0.06 per monomer unit of PnPA, PiPA, and PcPA, respectively. Because the *n*-propyl group has the largest A_{sf} of the three, the number of water molecules in its hydration shell is the largest. In addition, the number of hydrogen bonds per water molecule at its LCST is the largest because of the lowest LCST of the three. The ΔH of PnPA is, therefore, the largest, and the ΔH of PiPA is larger than that of PcPA.

Figure 10 shows the LCSTs of PnPA, PiPA, and PcPA in aqueous solutions containing one of the potassium halides (KF, KCl, KBr, and KI). The LCSTs are plotted against the value of $\Delta B = B_\eta - 0.0025V^0$ of the anions resulting from the salts, which represenst the strength of the interaction between the ions and water.[20] B_η and V^0 are the viscosity B coefficient and the partial molal volume of the anions, respectively. A linear relationship between the values of ΔB and the LCSTs was observed, but the slope of the line for PcPA was steeper than those for PnPA and PiPA.

To show the effects of the salts on the IR spectra, the profiles of the IR difference spectra of PnPA-d and PcPA-d in the presence and absence of NaCl are shown in Figure 11. To obtain the difference spectra, the IR

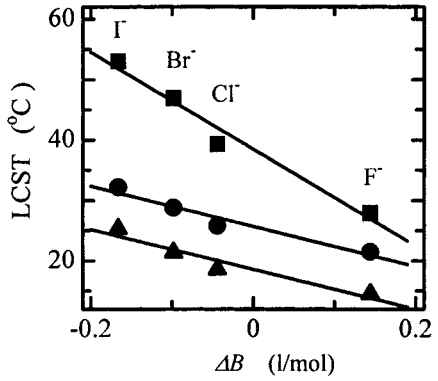

Figure 10. LCSTs of PnPA (▲), PiPA (●), and PcPA (■) in aqueous KF, KCl, KBr, and KI solutions ([salt] = 0.5 mol/L of solvent) measured by turbidimetry are plotted against $\Delta B = B_\eta - 0.0025V^0$ of the anions. The LCST was defined as the onset of absorption by the polymer solution (0.5 wt %) at 500 nm in the heating process (scanning rate = ca. 1 °C/min).

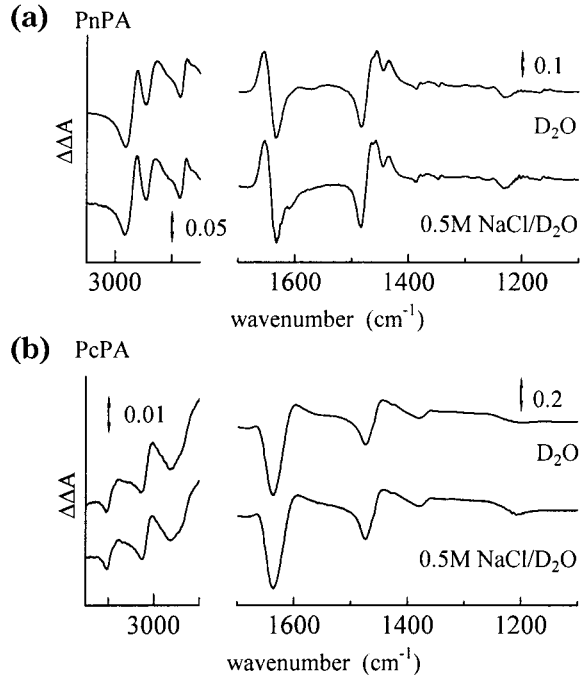

Figure 11. IR difference spectra of PnPA-d and PcPA-d (20 wt %) in D_2O measured in the presence and absence of NaCl. (a) IR difference spectra of PnPA-d in pure D_2O (top, $\Delta A_{26.5-22.0}$) and 0.5 mol/L of solvent NaCl/D_2O (bottom, $\Delta A_{17.1-12.1}$) (b) IR difference spectra of PcPA-d in pure D_2O (top, $\Delta A_{54.3-49.1}$) and 0.5 mol/L of solvent NaCl/D_2O (bottom, $\Delta A_{46.0-41.3}$).

absorption spectrum measured at the LCST of each polymer solution was subtracted from the spectrum measured near the LCST + 5 °C. The presence of NaCl did not influence the profiles of the IR spectra of the PnPA and PcPA solutions, although it does affect their LCSTs. The addition of the potassium halides to the solutions of PnPA and PcPA also had no effects on the profiles of the IR spectra of these polymers. The ineffectiveness of some metal halides on the profiles of the IR spectra of PiPA was also shown in a previous paper.[12] Thus, it is concluded that these kinds of metal halides have no influence on the IR spectra of these polymers.

There are several possibilities for the interaction between an ion and a neutral polymer including (1) direct interaction between the ion and a polar group on the polymer chain; (2) incorporation of the ion into the hydration shell of the polymer, which alters the water structure in the shell; and (3) exclusion of the ion from the hydration shell through repulsive interactions between the polymer and the ion, which causes a change in the water structure outside the shell. A cation has possibility of binding to the carbonyl oxygen, whereas an anion can interact with the N−H protons of the poly(*N*-alkylacrlyamide)s. If the carbonyl oxygen interacts with a cation, the amide I band, which is sensitive to hydrogen bonding and ion binding, might shift. If an anion binds to the amide proton, the amide II band might shift. Indeed, the carbonyl oxygen of *N*,*N*-dimethylformamide interacts with Na^+ and Li^+, and the amide I band shifts from 1675 cm^{-1} (bulk) to 1670 cm^{-1} ($NaClO_4$ solution) and 1665 cm^{-1} ($LiClO_4$ solution).[21] However, no detectable differences were observed in the amide bands of these polymers measured in the presence and absence of ions, although the LCSTs of the solutions were lowered. Therefore, direct interaction between the amide groups on the polymers and the ions is unlikely, and changes in the water structure in the hydration shells of the polymers is suggested instead.

Ions with $\Delta B > 0$ act as structure-makers for water, as their strong electrostatic interactions attract water molecules to them. On the other hand, ions with $\Delta B < 0$ are water structure-breakers, which break water−water hydrogen bonds but have such a weak electrostatic interaction with water that they do not hold water molecules. Water molecules around the ions with $\Delta B < 0$ move more rapidly than those in bulk water. Indeed, IR and Raman spectroscopic studies have shown that the number of water−water hydrogen bonds broken by potassium salts increases in the order $F^- < Cl^- < Br^-$.[22] The effectiveness of ions in the denaturation of proteins such as ribonuclease A is known to follow the Hofmeister or lyotropic series (F^-, 4.8; Cl^-, 10; Br^-, 11.1; I^-, 12.5).[23] Anions with higher lyotropic numbers lead to denaturation of proteins into coil-like structures, and those with lower numbers stabilize native structures (globule states). The denaturation of proteins and the phase transition of polymers observed here can be explained in a similar manner. Because anions with higher ΔB values or lower lyotropic numbers tend to subtract water molecules from polymers and proteins more strongly, they strengthen hydrophobic interactions that induced the collapse of polymers into the globule states. On the other hand, anions with lower ΔB values or higher lyotropic numbers break the structure of bulk water and stabilize hydrophobic hydration, so that the coil states are favored.

Conclusion

An IR spectroscopic study of the phase transitions of aqueous solutions of PnPA and PiPA revealed that the amide−water hydrogen bonding structure is partially broken and that the formation of intra- and interchain hydrogen bonds between the amide groups takes place during the coil-to-globule transition. However, most of the amide−water hydrogen bonds are retained even in the globule state of these polymers. The change in the profiles of the amide I′ band of PcPA during the transition was different from those of PnPA and PiPA. Although the amide I′ band of PcPA-d below the LCST was composed of single component assignable to C═O···D−O−D at 1634 cm^{-1}, two new components appeared at both the higher- and lower-wavenumber sides of the component. With an increase in temperature, the area of the 1634-cm^{-1} component decreased,

and the areas of the 1670-cm^{-1} and 1600-cm^{-1} components increased. The differences in the modes of hydrogen bonding of the amide groups in the globule states might be responsible for differences in their behaviors at the phase transitions. The effects of ions on the LCSTs of the polymers can be explained by the strengths of the interactions between the ions and water, that is, ions with higher ΔB values lower the LCST to a greater extent. Further systematic studies on the phase transitions of poly(*N*,*N*-dialkylacrylamide)s, poly(*N*-alkoxyacrylamide)s, poly(*N*-alkylmethacrylamide)s, and their copolymers are in progress in our laboratory. Details of the differences in the hydrogen bonding of the amide groups of these polymers will be discussed in forthcoming papers.

Acknowledgment. This work was supported by Grants-in-Aid (10750645, 12750795) from the Ministry of Education, Science and Culture, Japan. The authors are grateful to Shiseido Co., Tokyo, Japan, for financial support.

References and Notes

(1) (a) Liang, L.; Feng, X.; Liu, J.; Rieke, P. C.; Fryxell, G. E. *Macromolecules* **1998**, *31*, 7845. (b) Stayton, P. S.; Shimoboji, T.; Long, C.; Chilkoti, A.; Chen, G.; Harris, J. M.; Hoffman, A. S. *Nature* **1995**, *378*, 472. (c) Nozaki, T.; Maeda, Y.; Ito, K.; Kitano, H. *Macromolecules* **1995**, *28*, 522. (d) Kitano, H.; Maeda, Y.; Takeuchi, S.; Ieda K.; Aizu, Y. *Langmuir* **1994**, *10*, 403.

(2) Ptitsyn, O. B.; Kron, A. K.; Eizner, Y. Y. *J. Polym. Sci. C* **1968**, *16*, 3509.

(3) (a) Shirota, H.; Kuwabara, N.; Ohkawa, K.; Horie, K. *Macromolecules* **1999**, *103*, 10400. (b) Walter, R.; Rička, J.; Quellet, C.; Nyffenegger, R.; Binkert, T. *Macromolecules* **1996**, *29*, 4019. (c) Winnik, F. M. *Macromolecules* **1990**, *23*, 233.

(4) Terada, T.; Inada, T.; Kitano, H.; Maeda, Y.; Tsukida, N. *Macromol. Chem. Phys.* **1994**, *195*, 3261.

(5) (a) Ohta, H.; Ando, I.; Fujishige, S.; Kubota, K. *J. Polym. Sci., Polym. Phys.* **1991**, *29*, 963. (b) Tokuhiro, T.; Amiya, T.; Mamada, A.; Tanaka, T. *Macromolecules* **1991**, *24*, 2936.

(6) (a) Winnik, F. M.; Ottaviani, M. F.; Bossman, S. H.; Pan, W.; Garcia-Garibay, M.; Turro, N. J. *J. Phys. Chem.* **1993**, *97*, 12998. (b) Winnik, F. M.; Ottaviani, M. F.; Bossman, S. H.; Pan, W.; Garcia-Garibay, M.; Turro, N. J. *Macromolecules* **1993**, *26*, 4577. (c) Vesterinen, E.; Dobrodumov, A.; Tenhu, H. *Macromolecules* **1997**, *30*, 1311.

(7) (a) Tiktopulo, E. I.; Uversky, V. N.; Lushchik, V. B.; Klenin, S. I.; Bychkova, V. E.; Ptitsyn, O. B. *Macromolecules* **1995**, *28*, 7519. (b) Tiktopulo, E. I.; Bychkova, V. E.; Rička, J.; Ptitsyn, O. B. *Macromolecules* **1994**, *27*, 2879. (c) Feil, H.; Bae, Y. H.; Feijen, J.; Kim, S. W. *Macromolecules* **1993**, *26*, 2496. (d) Inomata, H.; Goto, S.; Otake, K.; Saito, S. *Langmuir* **1992**, *8*, 687. (e) Schild, H. G.; Muthkumar, M.; Tirrell, D. A. *Macromolecules* **1991**, *24*, 948. (f) Schild, H. G.; Tirrell, D. A. *J. Phys. Chem.* **1990**, *94*, 4352. (g) Otake, K.; Inomata, H.; Konno, M.; Saito, S. *Macromolecules* **1990**, *23*, 283.

(8) (a) Wang, X.; Qiu, X.; Wu, Chi. *Macromolecules* **1998**, *31*, 2972. (b) Qiu, X.; Kwan, C. M. S.; Wu, Chi. *Macromolecules* **1997**, *30*, 6090. (c) Meewes, M.; Rička, J.; Silva, M.; Nyffenegger, R.; Binkert, T. *Macromolecules* **1991**, *24*, 5811. (d) Kubota, K.; Fujishige, S.; Ando, I. *J. Phys. Chem.* **1990**, *94*, 5154. (e) Fujishige, S.; Kubota, K.; Ando, I. *J. Phys. Chem.* **1989**, *93*, 3311.

(9) Lee, L.-T.; Cabane, B. *Macromolecules* **1997**, *30*, 6559.

(10) Sasaki, S.; Koga, S.; Maeda, H. *Macromolecules* **1999**, *32*, 4619.

(11) (a) Ito, D.; Kubota, K. *Polym. J.* **1999**, *31*, 254. (b) Ito, D.; Kubota, K. *Macromolecules* **1997**, *30*, 7828. (c) Inomata, H.; Yagi, Y.; Saito, S. *Macromolecules* **1991**, *24*, 3962. (d) Inomata, H.; Yagi, Y.; Saito, S. *Macromolecules* **1990**, *23*, 4887. (e) Inomata, H.; Goto, S.; Saito, S. *Macromolecules* **1990**, *23*, 283.

(12) Maeda, Y.; Higuchi, T.; Ikeda, I. *Langmuir* **2000**, *16*, 7503.

(13) Rose, G. R.; Gezelowity, A. R.; Leser, G. J.; Lee, R. H.; Zehfus, M. H. *Science* **1985**, *226*, 834.

(14) Lele, A. K.; Hirve, M. M.; Badiger, M. V.; Mashelkar, R. A. *Macromolecules* **1997**, *30*, 157.

(15) (a) Tamai, Y.; Tanaka, H.; Nakanishi, K. *Macromolecules* **1996**, *29*, 6750. (b) Tamai, Y.; Tanaka, H.; Nakanishi, K. *Macromolecules* **1996**, *29*, 6761.

(16) Mizuno, K.; Ochi, T.; Shindo, Y. *J. Chem. Phys.* **1998**, *109*, 9502.

(17) Gu, Y.; Kar, T.; Scheuner, S. *J. Am. Chem. Soc.* **1999**, *121*, 9411.

(18) (a) Ide, M.; Maeda, Y.; Kitano, H. *J. Phys. Chem.* **1997**, *101*, 7022. (b) Hechet, D.; Tadesse, L.; Walters, L. *J. Am. Chem. Soc.* **1993**, *114*, 4336. (c) Hechet, D.; Tadesse, L.; Walters, L. *J. Am. Chem. Soc.* **1993**, *115*, 3336. (d) Hechet, D.; Tadesse, L.; Walters, L. *J. Am. Chem. Soc.* **1992**, *114*, 4336. (e) Green, G. L.; Sceats, M. G.; Lacey, A. R. *J. Chem. Phys.* **1987**, *87*, 3603. (f) Green, G. L.; Lacey, A. R.; Sceats, M. G. *Chem. Phys. Lett.* **1987**, *137*, 537. (g) Kitao, A.; Hirata, F.; Go, M. *J. Phys. Chem.* **1993**, *97*, 10223.

(19) (a) Walrafen, G. E. *J. Chem. Phys.* **1968**, *48*, 244. (b) Walrafen, G. E. *J. Chem. Phys.* **1966**, *44*, 1546.

(20) Desnoyers, J. E.; Perron, G. *J. Solution Chem.* **1972**, *1*, 199.

(21) Bukowska, J. *J. Mol. Struct.* **1983**, *98*, 1.

(22) (a) Verrall, R. E. In *Water A Comprehensive Treatise*; Frank, F., Ed.; Plenum Press: New York, 1975; Vol. 3, p 211. (b) Terpsta, P.; Combes, D.; Zwick, A. *J. Chem. Phys.* **1990**, *92*, 65.

(23) (a) McBain, J. W. In *Colloid Science*; Heath: Boston, MA, 1950. (b) Robinson, D. R.; Jencks, W. P. *J. Am. Chem. Soc.* **1965**, *87*, 2470.

MA001306T